Int J Biochem Mol Biol 2024;15(2):20-33
www.ijbmb.org /ISSN:2152-4114/IJBMB0154788

Original Article

Biophysical characterization and insights into the oligomeric nature of CD2-associated protein

Abrar H Qadri[1], Jyotsana Prajapati[1], Iqball Faheem[2], Utsa Bhattacharjee[1], Hari Krishnan Padmanaban[1], Sandeep KN Mulukala[1], Anil K Pasupulati[1]

[1]*Department of Biochemistry, University of Hyderabad, Hyderabad 500046, India;* [2]*Department of Microbiology and Cell Biology, Indian Institute of Science, Bangalore 560012, India*

Received December 5, 2023; Accepted February 27, 2024; Epub April 15, 2024; Published April 30, 2024

Abstract: Introduction: Glomerular podocytes are specialized epithelial cells localized to the blood-urine interface of the kidney. Podocyte slit-diaphragm (SD), a size-and-charge-selective junction, is instrumental in blood ultrafiltration and the formation of protein-free urine. The SD consists of macromolecular complexes of several proteins, such as nephrin, podocin, and CD2-associated protein (CD2AP). CD2AP is an adapter protein and is considered to be crucial for the integrity of SD. Mutations in the SD proteins cause nephrotic syndrome (NS), characterized by proteinuria. SD proteins' structural features must be elucidated to understand the mechanism of proteinuria in NS. In this study, we expressed, purified, and biophysically characterized heterologously expressed human CD2AP. Methods: Codon-optimized human CD2AP was expressed in *E. coli* Rosetta cells. The recombinant protein was induced with 1 mM IPTG and purified by Ni-NTA affinity chromatography. Analytical size-exclusion chromatography, blue native-PAGE, circular dichroism, and fluorescence spectroscopy were performed to decipher the oligomeric nature, secondary structural content, and tertiary packing of CD2AP. Results: Our analysis revealed that CD2AP adopts a predominantly disordered secondary structure despite exhibiting moderate tertiary packing, characterized by low helical and β-sheet content. CD2AP readily assembles into homo-oligomers, with octamers and tetramers constituting the primary population. Interestingly, the inherent flexibility of CD2AP's secondary structural elements appears resistant to thermal denaturation. Frameshift mutation (p.K579Efs*7) that leads to loss of the coiled-coil domain promotes aberrant oligomerization of CD2AP through SH3 domains. Conclusion: We successfully expressed full-length human CD2AP in a heterologous system, wherein the secondary structure of CD2AP is predominantly disordered. CD2AP can form higher-order oligomers, and the significance of these oligomers and the impact of mutations in the context of size-selective permeability of SD needs further investigation.

Keywords: CD-2 associated protein, slit-diaphragm, podocyte, kidney, nephrotic syndrome, proteinuria

Introduction

Kidneys are indispensable organs with the crucial function of efficiently excreting metabolic waste products and toxins [1, 2]. They also play a vital role in regulating electrolyte, water, and acid-base balance, which are critical for maintaining body homeostasis [3]. Nephron, the functional unit of the kidney, has two regions: the glomerulus and the tubule [4]. The glomerulus selectively permits the passage of small molecules like water, amino acids, and urea while restricting larger macromolecules like albumin and antibodies, thus tightly controlling the composition of urine [5, 6]. This selective filtration is achieved through the glomerular filtration barrier (GFB), composed of fenestrated endothelial cells, glomerular basement membrane (GBM), and the outermost layer of podocytes [7]. The GFB represents the kidney's filtration function. Podocytes stand out among the three crucial components of GFB due to their specialized functional and structural features [7-9]. These cells possess a network of intricate protrusions known as foot processes, further classified as primary and secondary foot processes [10, 11]. Notably, the interdigitating secondary foot processes of adjacent podocytes are linked by a modified tight-and-adherens junction called the slit diaphragm (SD) [12, 13]. This specialized structure acts as a molecular sieve of approximately 30-40 nm, effectively fil-

https://doi.org/10.62347/UVSH8436

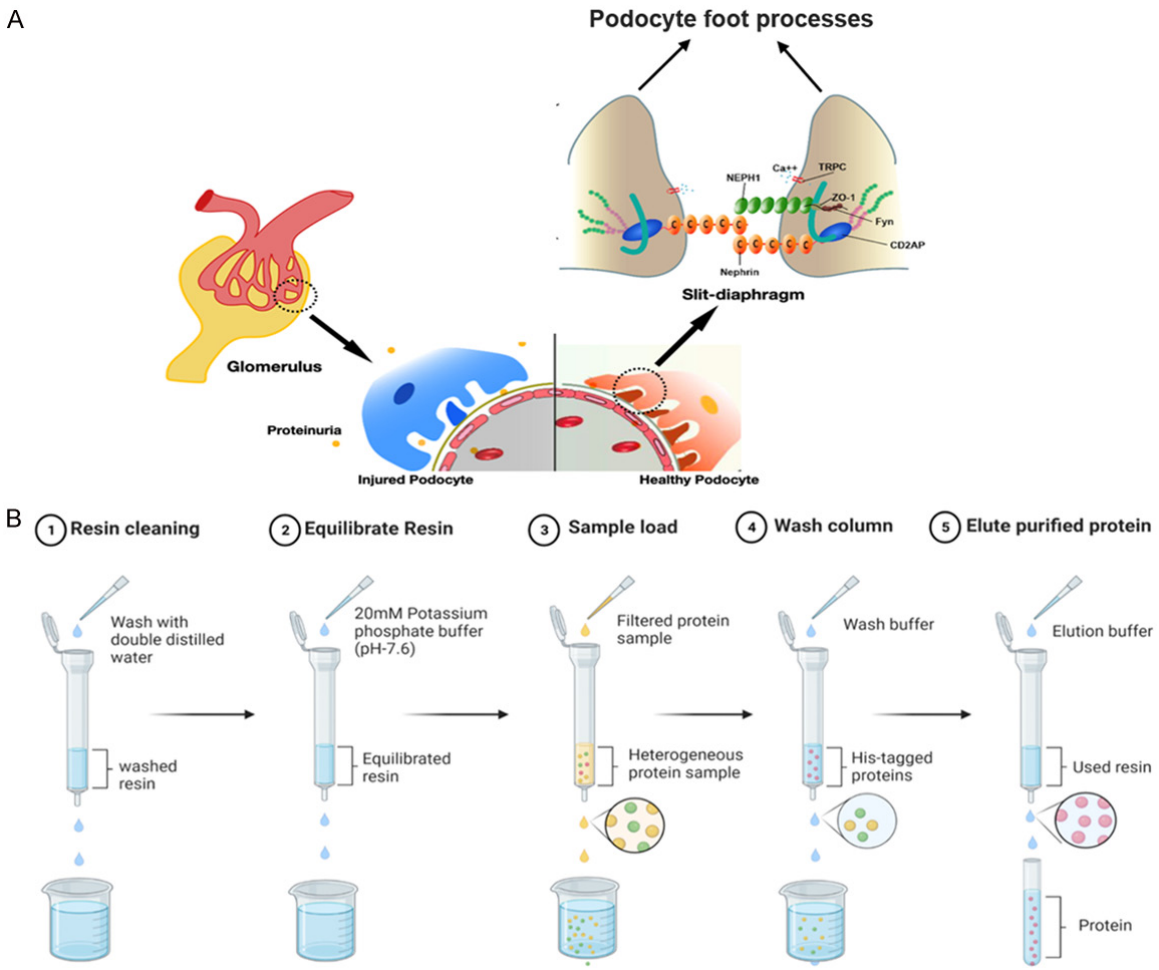

Figure 1. Schematic representation of podocyte slit-diaphragm. A. The glomerulus is a filtration part of the kidney. Podocytes are major cell types that represent the filtration apparatus. Slit-diaphragm, a macromolecular assembly of several proteins, including CD2AP, forms the blood-urine barrier. B. Cartoon depicting affinity purification protocol for N-terminal His-tag CD2AP expressed in *E. coli*. The supernatant of bacterial lysate is loaded onto an equilibrated 5 ml HisTrap column (Cytiva), washed with 20 mM potassium phosphate buffer pH 7.6, 50 mM NaCl, 5% glycerol, and 100 mM imidazole and then eluted with 20 mM potassium phosphate pH 7.6, 50 mM NaCl, 5% glycerol, 400 mM imidazole.

tering small molecules while retaining larger molecules within the blood [9, 10].

The SD is a negatively charged zipper-like structure spanning 30-40 nm between the adjacent foot processes of podocytes (**Figure 1A**) [12, 13]. The negative charge of podocyte SD and its ability to serve as a tight-and-adherens junction is due to the macromolecular assembly of constituent proteins, including CD-2 associated protein (CD2AP), nephrin, podocin, nephrin-like proteins 1, 2, and 3 (NEPH), transient receptor potential cation channel (TRPC6), and zonula occludens (ZO-1) (**Figure 1A**) [14-19]. The SD proteins are extracellular (e.g., Nephrin), membrane-associated (e.g., Podocin), transient channels (e.g., TRPC6), and also serve as adapters (e.g., CD2AP) [20]. Podocyte SD prevents the transit of negatively charged albumin from the blood into the urinary space and tightly regulates urine composition. The structural details, precise assembly, and stoichiometry of the SD proteins, including CD2AP, are of great concern to nephrologists [12, 13, 21, 22]. CD2AP, which is expressed and localized to podocyte foot processes, ensures the integrity of the SD through interactions with other essential podocyte proteins like nephrin, podocin, and TRPC6 [16, 23] (**Figure 1A**). Besides its structural role, CD2AP also participates in signal transduction [24]. Mutations in CD2AP lead to podocyte apoptosis, deficiencies in endocy-

tosis, and vesicle trafficking [25-27]. CD2AP knockout mice develop severe NS and focal-segmental glomerulosclerosis (FSGS) and have short lifespans [28, 29]. Mutations in CD2AP are also associated with NS and FSGS [28-30]. Patients with mutations in the CD2AP gene are characterized by proteinuria, hypoalbuminemia, and edema [31, 32].

Although multiple studies indicate the essential role of CD2AP in normal renal function and NS patients, the precise role of CD2AP in the architecture of SD remains unexplored [12]. Furthermore, the mechanism for mutations' effect on proteinuria needs to be investigated [29, 33, 34]. Earlier investigations into the structural details of CD2AP are very scant [35] and confined to the protein's short regions [36]. In this study, we successfully expressed and purified full-length human CD2AP. We subsequently investigated its oligomeric nature, evaluated the secondary structural content and its structural stability. Further, we predicted the effects of a frameshift insertion mutation on CD2AP structure and oligomerization.

Results

Heterologous expression and purification of human CD2AP

A codon-optimized CD2AP construct was purchased and overexpressed in *E. coli* Rosetta (DE3). The entire protocol of CD2AP purification is depicted in **Figure 1B**. Due to intrinsically disordered regions (IDRs), the protein aggregates and accumulates in inclusion bodies. To enhance the CD2AP expression, we optimized the IPTG concentration and the post-induction incubation temperature. With an IPTG concentration of 1 mM and an optimal induction time of 16 hours at 14°C, we observed a significant increase in protein expression compared to uninduced cultures (**Figure 2A**). The composition of buffers to purify this protein and prevent precipitation is provided in the methods section. We employed a single-step Ni-NTA affinity chromatography to purify the protein (**Figure 2B**) from *E. coli* Rosetta (DE3) lysates overexpressing CD2AP. This protocol yielded substantial amounts (~15 mg/L of culture) of full-length soluble CD2AP, sufficient for the biophysical characterization.

CD2AP adopts multi-oligomeric states

CD2AP and other SD proteins form a vast network of protein-protein interactions. To understand CD2AP's role in these interactions, evaluating its stability and oligomeric nature is essential. We subjected CD2AP to analytical size exclusion chromatography (SEC) using a Superdex 200 10/300 column. CD2AP eluted at 9 ml, the boundary between void and elution volumes (Supplementary Figure 1A). SDS-PAGE analysis confirmed the presence of intact CD2AP in these fractions (Supplementary Figure 1B). To further determine whether CD2AP exists as an aggregate or a higher-order oligomer, we resolved CD2AP on a Superose 6 10/300 column. CD2AP eluted as overlapping peaks (**Figure 3A**). Deconvolution of the chromatogram using multi-peak fit analysis revealed peaks at 10 ml, 11 ml, 12.8 ml, and 20.3 ml (**Figure 3B**). SDS-PAGE analysis of peak fractions confirmed the presence of CD2AP in the first three peaks (**Figure 3C**). This data suggests that CD2AP could exist in various oligomeric states. We then compared the elution profiles of CD2AP and blue dextran to rule out the possibility of CD2AP forming aggregates (Supplementary Figure 2). The peak at 10 ml in the CD2AP chromatogram corresponds to higher-order oligomers and not aggregated CD2AP. Peaks at 11 ml and 12.8 ml signify well-defined lower oligomeric forms, and the prominent peak at 20.3 ml may suggest degradation products of CD2AP, as no protein bands were observed in SDS-PAGE (**Figure 3C**).

We subsequently performed Blue Native-Polyacrylamide Gel Electrophoresis (BN-PAGE) to estimate the molecular weight of different oligomeric forms of CD2AP. The BN-PAGE analysis of the affinity-purified CD2AP samples revealed that CD2AP adopts two predominant oligomeric conformations, including octamers (~559 kDa) and tetramers (~294 kDa) (**Figure 3D**). These results align with our SEC data, suggesting that the three bands in BN-PAGE may represent the individual peaks (peaks 1,2,3) in the chromatogram (**Figure 3A** and **3B**). These findings imply CD2AP adopts higher-order oligomeric conformations, potentially as octameric and tetrameric forms when isolated. Furthermore, CD2AP is relatively unstable, partly due to the absence of post-translational modifications and binding partners.

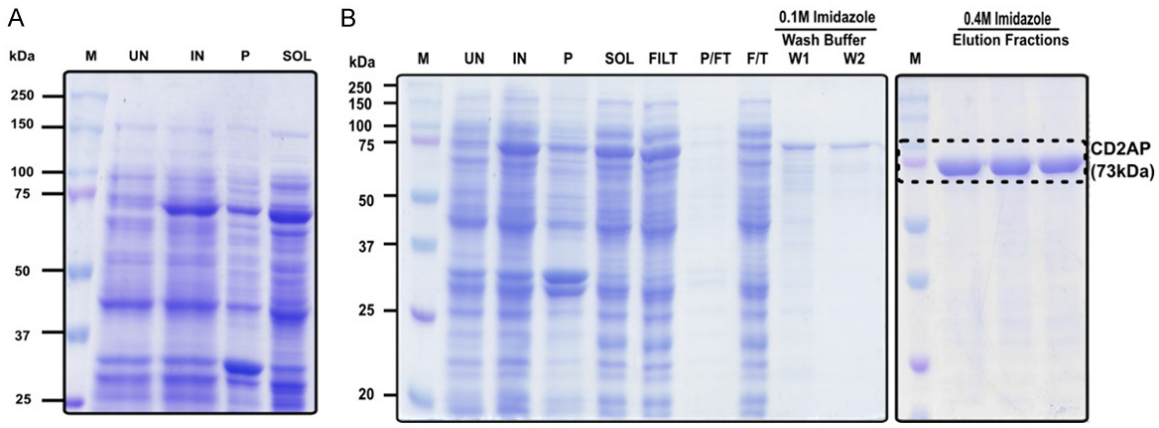

Figure 2. Expression and Purification of CD2AP by affinity chromatography. A. SDS-PAGE analysis of cell lysates from uninduced and induced bacterial cell strain Rosetta (DE3) containing pET28a *CD2AP*. B. SDS-PAGE of different fractions from Ni-NTA affinity chromatography of CD2AP protein. M = marker, UN = un-induced, I = Induced, P = pelleted cell debris, Sol = soluble lysate, Filt = Filtrated Sol. fraction, P/FT = pre-flow through, FT = flow through, W1 = Wash1, W2 = Wash2, E = Elution fractions.

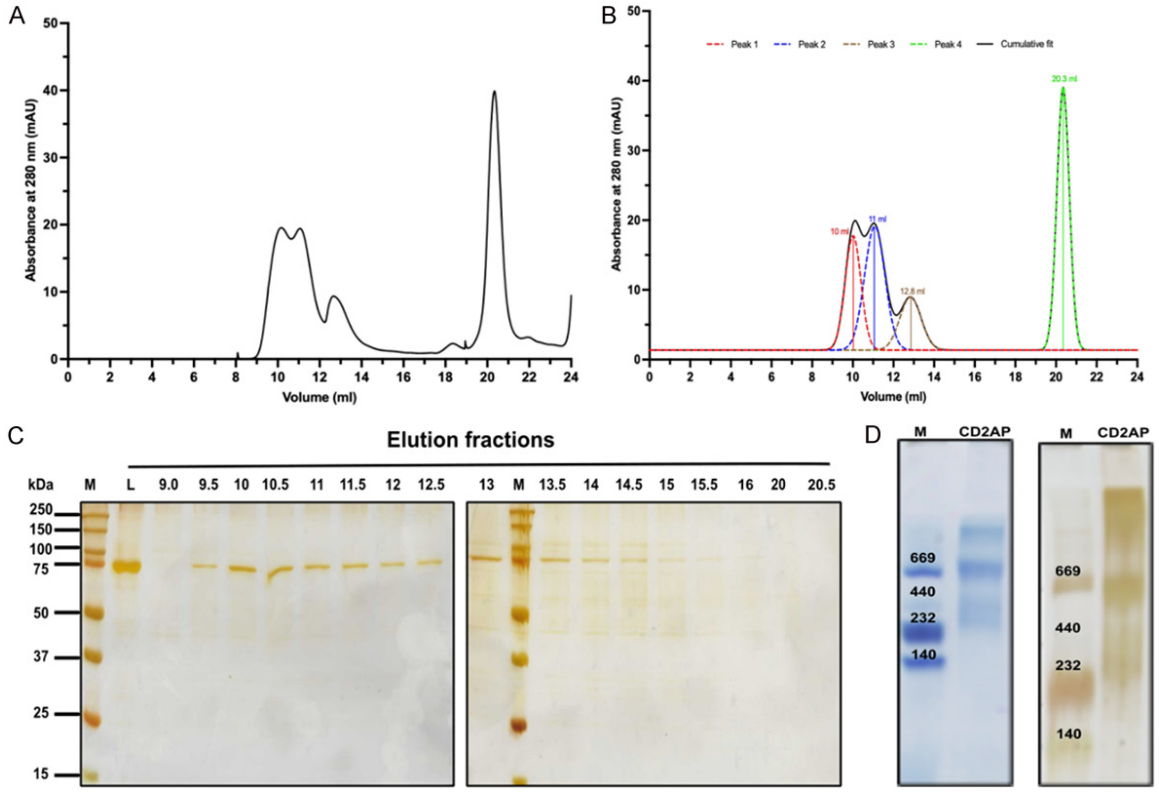

Figure 3. CD2AP adopts multi-oligomeric states. A. Gel filtration chromatogram showing different oligomeric states adapted by CD2AP. B. A deconvoluted gel filtration chromatogram shows possible elution peaks of different CD2AP oligomers at 10 ml, 11 ml, 12.8 ml, and 20.3 ml, respectively. C. SDS-PAGE analysis of the fractions collected from the gel filtration chromatogram. D. Blue native gel electrophoresis (BN-PAGE) of the purified CD2AP.

Secondary and tertiary packing of CD2AP

Despite CD2AP adopting various oligomeric conformations, we were interested in examining the protein's secondary structural elements and tertiary packing. To assess the secondary structural properties of CD2AP, we analyzed the far-UV Circular Dichroism (CD) spectra of

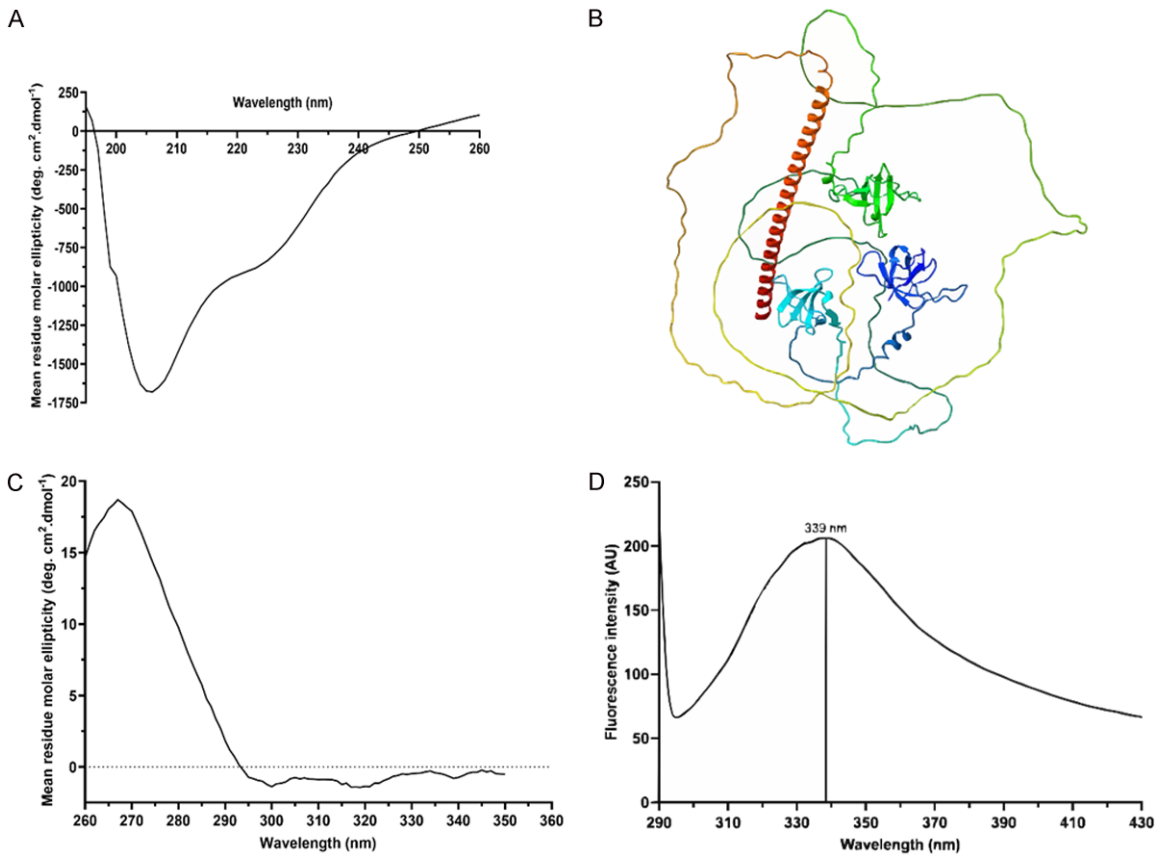

Figure 4. Secondary structural elements and tertiary packing of CD2AP. A. Far-UV CD spectrum (195 nm-260 nm) representing the secondary structural content of CD2AP. B. Alpha Fold predicted model of full-length human CD2AP. C. Near-UV CD spectrum (260 nm-360 nm) representing the tertiary packing of CD2AP. D. Fluorescence emission spectrum (290 nm-430 nm) of the CD2AP recorded by exciting the protein at 286 nm.

SEC-purified samples. We observed pronounced minima spanning 200-215 nm, suggesting the presence of random coils and beta-sheets, along with a alpha-helical signature at 222 nm (**Figure 4A**). To better understand this unique spectrum, we examined the predicted structure of CD2AP from AlphaFold (**Figure 4B**). The structural details reveal that large portions of CD2AP are essentially random coils, except for the SH3 domains, which consist of beta-sheets and a significant C-terminal helix (**Figure 4B**). The helical signature at 222 nm in our spectra may correspond to the C-terminal helix in the model. Thus, far-UV CD experiments suggest that random coils dominate the secondary structure of CD2AP, followed by beta-sheets and helices.

Next, we investigated the tertiary packing of CD2AP using near-UV CD spectroscopy and tryptophan fluorescence. In the near-UV CD spectrum, a broad signal spanning approximately 260-297 nm suggests the existence of the protein's tertiary structure (**Figure 4C**). Similarly, the tryptophan fluorescence spectrum of CD2AP exhibited a strong signal with a peak intensity at 339 nm (**Figure 4D**). Therefore, it can be concluded that CD2AP, in isolation, attains a considerable secondary structure and tertiary packing; however, intrinsically unstructured regions dominate the secondary structure.

Structural stability of CD2AP

Despite CD2AP exhibiting moderate secondary and tertiary packing, we were interested in exploring its structural stability. We subjected the protein to a temperature range from 4°C to 90°C and analyzed the structural changes by measuring CD spectra at the respective temperatures (**Figure 5A**). As the temperature increased, the signal intensity at wavelengths 205 nm and 222 nm, corresponding to random

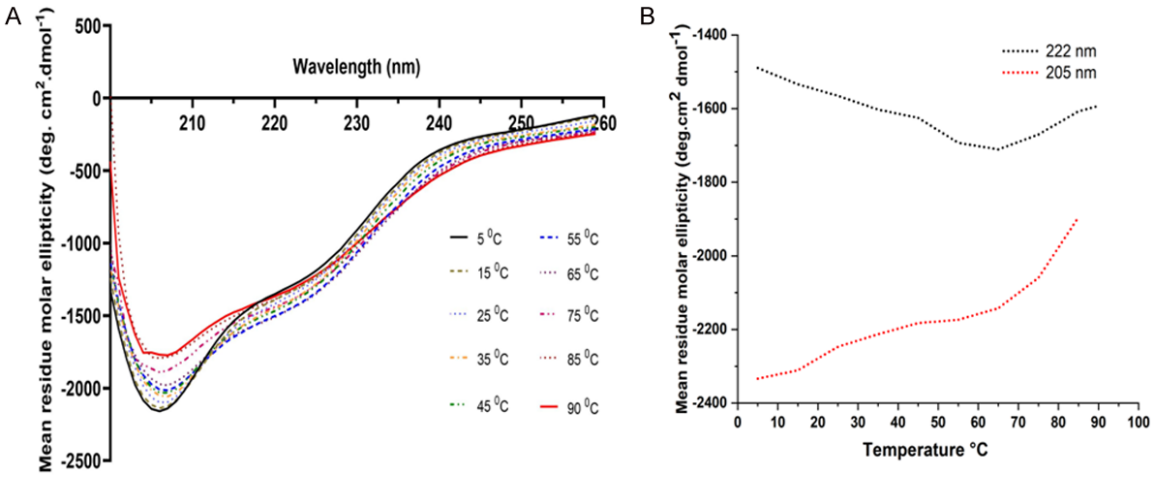

Figure 5. Assessing the stability of secondary structural elements of CD2AP oligomers. A. Far-UV spectra (260-200 nm) of the CD2AP protein plotted as a function of temperature (5°C-90°C). B. The MRE values of the CD2AP protein at 222 nm and 205 nm were plotted against increased temperature to monitor the changes in protein structure.

coils and helix signatures, showed minimal changes (**Figure 5B**). Interestingly, at 222 nm, the signal intensity increased temperature upto 65°C and changed minimally beyond 65°C. Moreover, the signals corresponding to sheets, helices, and random coils never reduced to zero, even at higher temperatures. These results suggest that secondary structures of CD2AP are stable at higher temperatures.

The fluorescence emission spectrum of proteins, often attributed to tryptophan and tyrosine residues, can offer insights into changes induced in a protein's secondary or tertiary structure. Therefore, we examined temperature-induced structural alterations in CD2AP by measuring changes in the fluorescence emission spectra. CD2AP protein contains 5 Trp and 11 Tyr residues. As a result, a characteristic fluorescence spectrum was observed, with its peak intensity at 5°C indicating partial exposure of the Trp residue to the solvent environment at this temperature (**Figure 6A**). Furthermore, the spectra show a uniform decrease in intensity with increasing temperature (**Figure 6B**). The change in fluorescence intensity as a function of temperature shows a linear transition rather than a sigmoidal shape, typically observed for proteins with a tightly packed tertiary core (**Figure 6B**). Subsequently, we reversed the temperature changes and examined the fluorescence spectra at various intervals of decreasing temperature (from 95°-5°C). The fluorescence intensity increased with gradual cooling, indicating protein refolding (**Figure 6C** and **6D**). However, the pattern of fluorescence spectra with decreasing temperature did not completely reciprocate the spectra observed during the temperature-dependent unfolding of the protein (**Figure 6C** and **6D**). The data suggests that a thermally perturbed state of CD2AP only partially returns to its native state (Supplementary Figure 4). We also monitored the fluorescence emission spectrum of CD2AP in response to increasing urea concentrations since podocyte SD is constantly exposed to nitrogenous waste products. The fluorescence spectra depicted the structural stability of CD2AP up to 1M urea concentration, with complete denaturation beyond 3M (Supplementary Figure 3). Together, these results reveal higher stability of the structural organization of CD2AP at supraphysiological conditions attributed to the dominance of IDRs.

*Impact of mutation (p.K579Efs*7) on CD2AP oligomerization*

CD2AP subunit comprises three SH3 domains, polyproline region, carmil peptide region, and C-terminal coiled region (**Figure 7A**). We employed AlphaFold to verify whether any conformational difference exists between the CD2AP monomer and an individual subunit of the CD2AP tetramer. Alphafold predicted alternate conformations for monomeric and tetrameric CD2AP subunits with a Root Mean Square Deviation (RMSD) value of 47.842 Å (computed

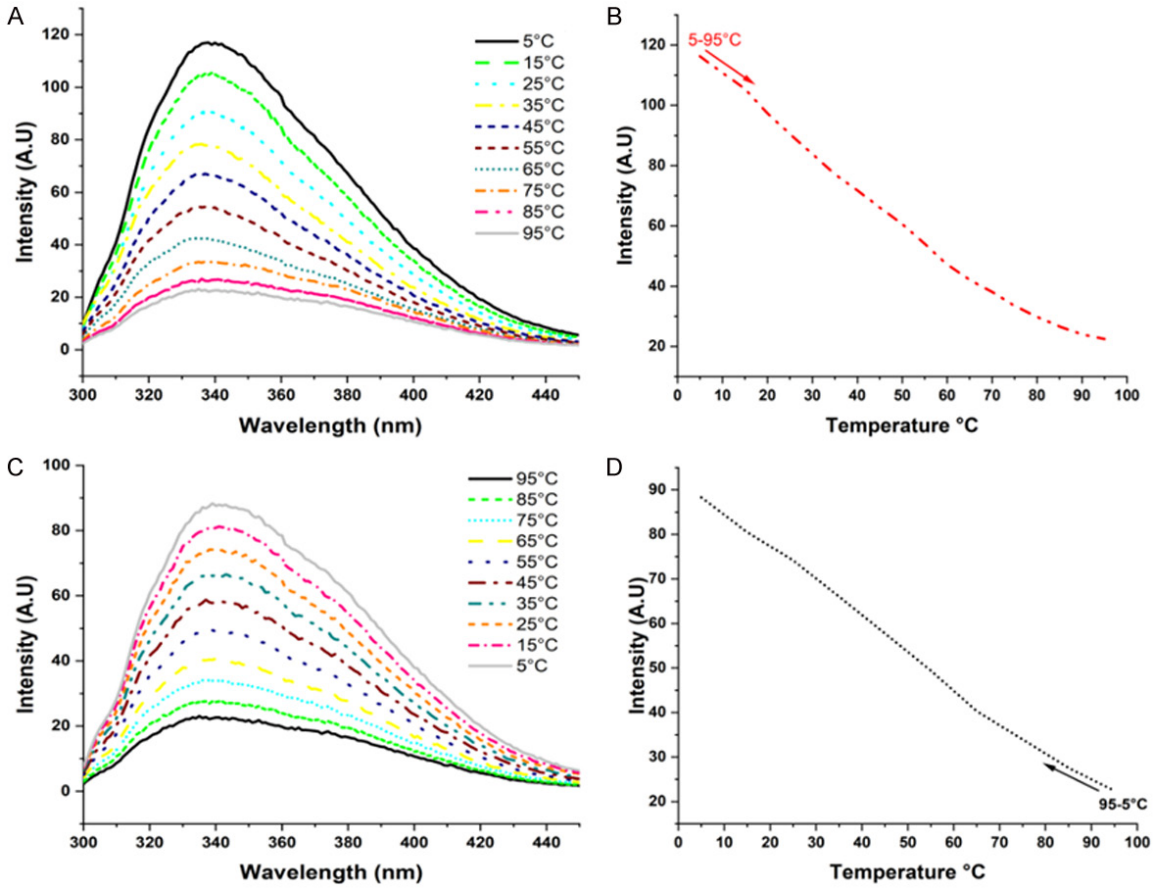

Figure 6. Assessing the stability of the tertiary structure of CD2AP oligomers. A. Intrinsic tryptophan fluorescence for CD2AP protein was measured and plotted as a function of temperature (5°C-90°C) by exciting the protein at 286 nm. B. Peak emission of the CD2AP protein at 339 nm is plotted over a temperature range of (5°C-90°C). C. To track the protein refolding, intrinsic tryptophan fluorescence for CD2AP protein was measured as a function of temperature (95°C-5°C) by exciting the protein at 286 nm. D. Peak emission of the CD2AP protein at 339 nm is plotted over a temperature range of (95°C-5°C).

on the 636 Cα atoms aligned). The modeled tetramer of CD2AP oligomerizes via a C-terminal coiled-coil region (**Figure 7B** and **7C**). The predicted interactions indicate that 66 residues of each subunit, of which 48 belong to the coiled-coil domain, are involved in interactions. In the CD2AP tetramer (B, C, D, & E), residues from the B and D chains interact with residues from the C chain via salt bridges and hydrogen bonds (**Figure 7D**). A frameshift insertion mutation (p.K579Efs*7) in the CD2AP gene leads to a truncation of the CD2AP at the predicted interacting interface (**Figure 7A**). The generated tetrameric mutant model was shown to oligomerize through its SH3 domains due to the loss of the coiled-coil domain (**Figure 8A** and **8B**). The results suggested that residues from all three SH3 domains of all the subunits could be involved in interactions within the complex (**Figure 8C**).

Discussion

The podocyte SD has garnered significant attention due to its unique structural features and its crucial role in kidney filtration [5, 9, 12]. The proper functioning of the SD relies on the structural integrity of individual SD proteins and their association as large macromolecular complexes, as mutations in these proteins can lead to severe proteinuria [30]. CD2AP, a critical protein localized to the SD, is a scaffolding-adaptor protein [34, 37]. CD2AP, while interacting with its neighboring SD proteins, forms a physical link with the actin cytoskeleton of podocytes, thus participating in numerous signaling pathways and aiding the SD's structural integrity [5, 24, 38]. Several studies affirm a decisive role for CD2AP, and mutations in CD2AP have been reported to impact the structural integrity and architecture of the SD [6, 28,

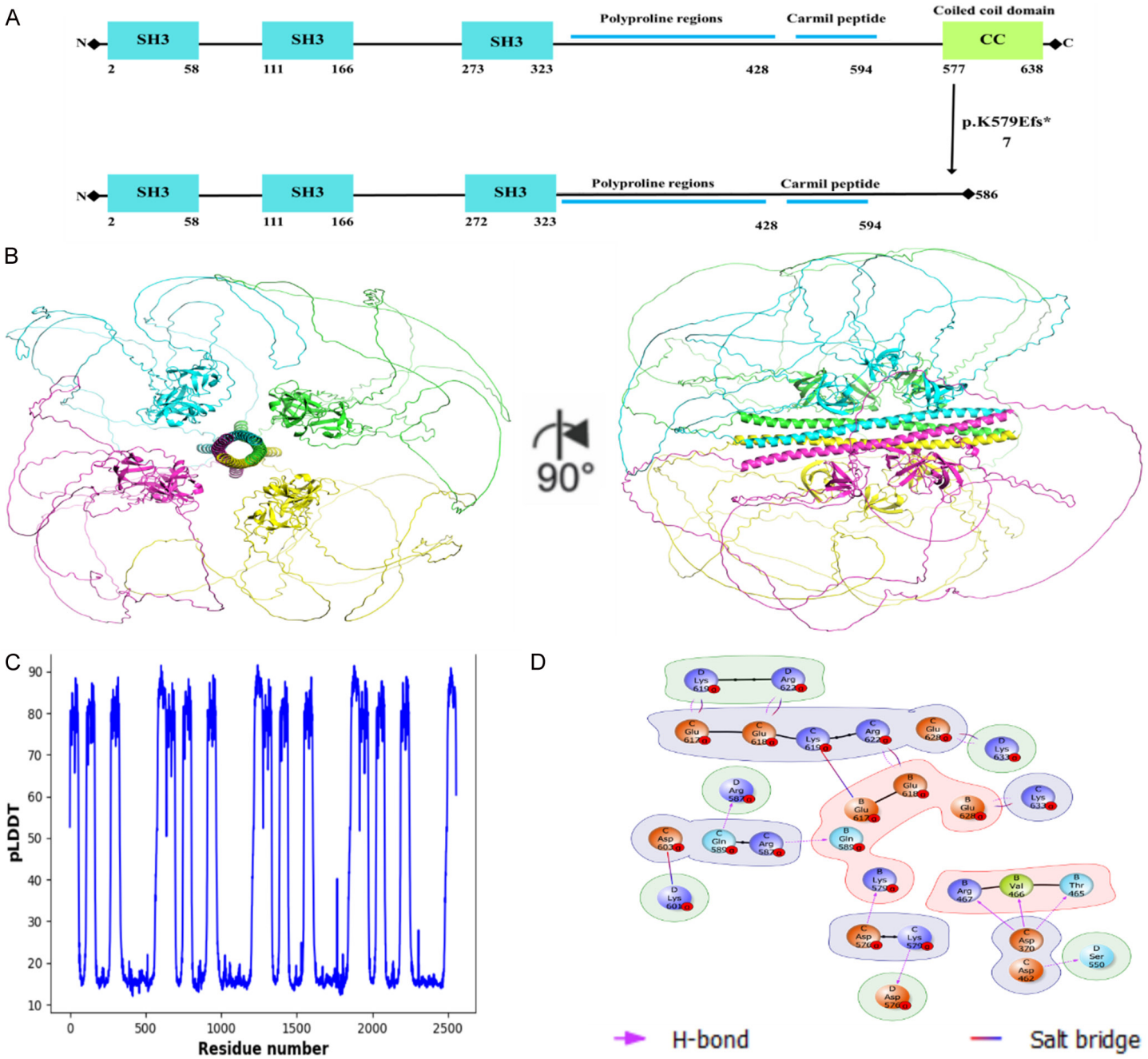
A
N
SH3
SH3
SH3
Polyproline regions
Carmil peptide
Coiled coil domain
CC
C
2
58
111
166
273
323
428
594
577
638
p.K579Efs*
7
586
272
B
90°
C
pLDDT
Residue number
D
H-bond
Salt bridge

Figure 7. Structural features of CD2AP. A. Schematic representation of CD2AP (WT and p.K579Efs*7). SH3 - Src homology 3 domains; CC - Coiled-coil domain. B. A cartoon illustration of the predicted full-length model of the wild-type CD2AP tetramer, colored by a chain. C. The AF per-residue confidence measure (pLDDT) represents the structural model. D. The expected salt bridges and hydrogen bonds between chains B and D with C within the tetramer are depicted graphically.

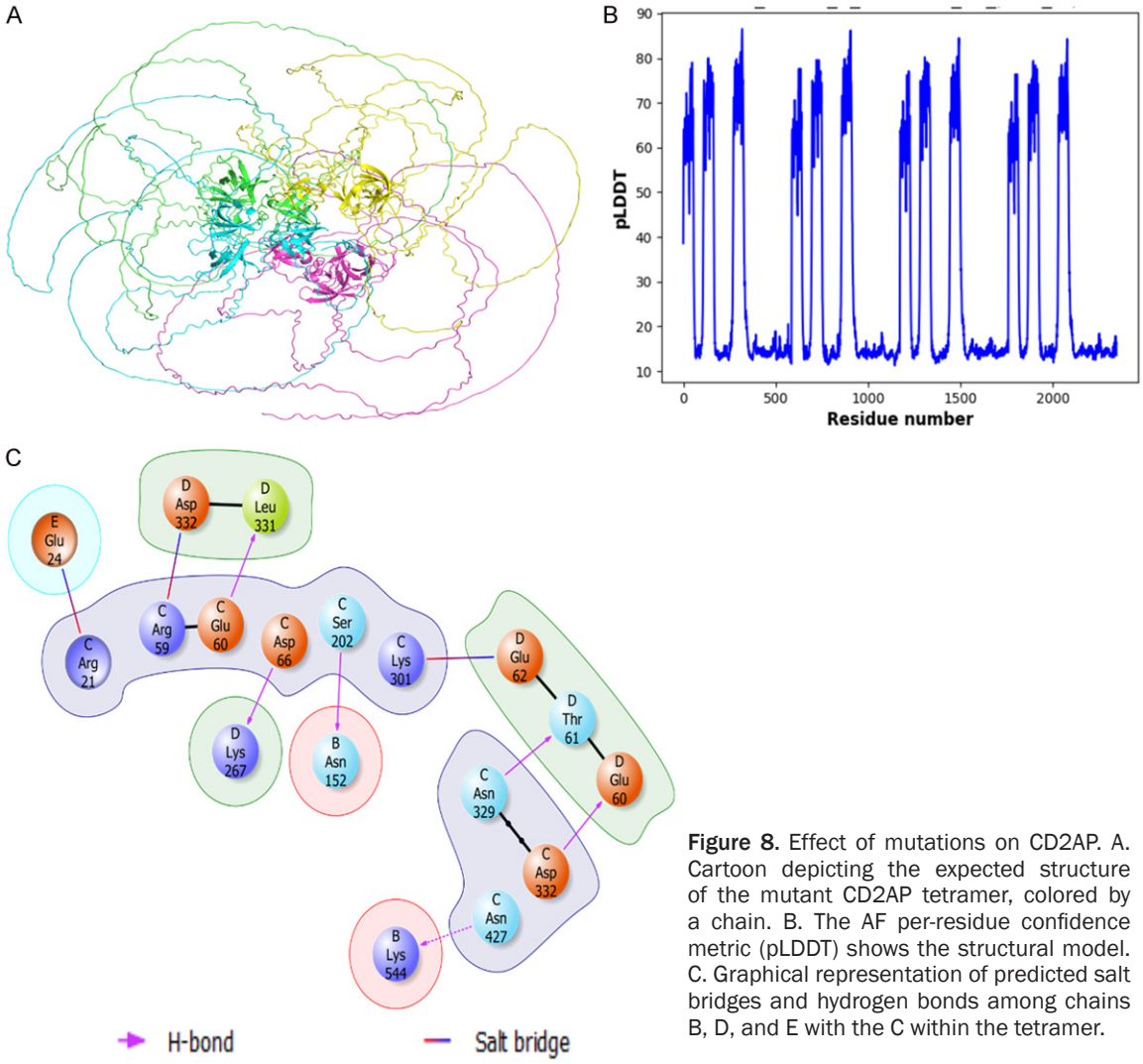

Figure 8. Effect of mutations on CD2AP. A. Cartoon depicting the expected structure of the mutant CD2AP tetramer, colored by a chain. B. The AF per-residue confidence metric (pLDDT) shows the structural model. C. Graphical representation of predicted salt bridges and hydrogen bonds among chains B, D, and E with the C within the tetramer.

39, 40]. One challenge hindering the structural characterization of CD2AP was the lack of a unified purification protocol capable of yielding sufficient amounts of the protein. In this study, we standardized the protocol to successfully express the recombinant human CD2AP and purify it from *E. coli*. This study shows that CD2AP, in isolation, adopts octameric and tetrameric configurations. CD2AP has a greater tendency to form higher-order oligomers. Further, by employing CD and tryptophan fluorescence, we show that CD2AP secondary structure is majorly IDRs with moderate tertiary and quaternary packing. Moreover, we predicted the impact of frameshift insertion mutation (p.K579Efs*7) [34] on CD2AP oligomerization.

Our Size Exclusion Chromatography (SEC) and Blue Native Polyacrylamide Gel Electrophoresis (BN-PAGE) results indicate that CD2AP exists in tetrameric, octameric, and higher-order oligomeric states. Our findings correlate with the tetrameric oligomers observed by Adair et al. [35]. The higher oligomeric states observed in our study may arise due to the absence of interacting partners and molecular crowding, which

may differ from physiologically relevant conditions. The C-terminal coiled-coil (CC) region is essential for CD2AP's oligomerization; CD2AP without the CC region failed to oligomerize [41]. In contrast, the customarily truncated CD2AP C-terminal CC formed trimers in the solution [41]. A frameshift insertion mutation (p.K579Efs*7) resulted in a truncated form of CD2AP devoid of CC region [34]. Our data suggests that this truncated form of CD2AP oligomerizes via the SH3 domain instead of the CC region. CD2AP's inherent ability to form oligomers and its potential to serve as a scaffold molecule may be distorted by mutations that result in the loss of SD's architecture and proteinuria [41]. It has been confirmed that CD2AP interacts with several SD proteins and cytoskeletal proteins. Monomeric or lower-order oligomeric forms of wild-type or mutant CD2AP may be incapable of forming a large protein complex crucial for maintaining SD architecture and permselectivity. In addition to associating as hetero-oligomers, most SD proteins can form large oligomers, and these interactions are facilitated by IDRs [23, 41-46]. SD proteins in higher oligomeric forms are crucial in mediating, stabilizing, and achieving 30-40 nm pore dimensions.

Previously, we predicted that 65-75% of CD2AP is intrinsically disordered [41]. CD further substantiates the intrinsic disorderliness in CD2AP. A pronounced negative minima around 200 nm supports our assertion that IDRs dominate the secondary structural content in CD2AP, followed by sheets and helices. We investigated the temperature dependence of CD spectra from 5 to 90°C, revealing a significant increase in negative ellipticity around 222 nm and a decrease around 200 nm. These findings suggest heat-induced folding of the peptide chain into α-helices and β-sheets [47, 48]. Studies show several signaling and regulatory proteins have IDRs [43, 49-52]. These IDRs are vital in mediating and facilitating multivalent electrostatic interactions, which are crucial to initiate and sustain the formation of macromolecular complexes within the SD [42, 53].

Conclusion

In this study, we detailed the heterologous expression, solubilization, and purification of full-length recombinant human CD2AP. We showed that CD2AP exists in higher-order oligomeric conformations, especially octameric and tetrameric forms. The data revealed that IDRs with modest tertiary packing dominate the protein in isolation. This study speculated how a mutation in a CD2AP may affect its oligomeric state and possibly the entire SD architecture. To further garner clues about CD2AP structure and its oligomers, we propose to carry out analytical centrifugation and small-angle X-ray scattering analysis.

Materials and methods

Construction of CD2AP expression vector

The *CD2AP* gene was cloned into a pET28a (+) vector purchased from Genscript (Piscataway, New Jersey, USA). The vector is 5.4 kb and carries an N-terminal 6X-His tag, kanamycin resistance, a *lac I* gene, a T7 terminator, and a thrombin cleavage site. The gene was inserted between the Nde1 and Xho1 sites. The expression vector was then transformed into the *E. coli* Rosetta (DE3) strain for overexpression of CD2AP.

Induction and expression of CD2AP

Secondary culture (16 hrs at 4°C) of the CD2AP transformed *E. coli* was induced with 1 mM Isopropyl-β-D thiogalactopyranoside (IPTG). The culture was centrifuged (8000 rpm) for 20 min at 4°C, the supernatant was discarded, and the pellet was stored at -20°C. Pellet was resuspended in lysis buffer A (20 mM potassium phosphate, 50 mM NaCl, 5% glycerol-pH 7.6) (all reagents are from Sigma Aldrich, Italy) supplemented with 0.1% triton X-100 (SRL), a protease inhibitor cocktail (Roche, Germany), and 0.1 mg/ml lysozyme (Himedia). The suspension was sonicated (29 sec ON, 59 sec OFF) in ice and centrifuged (12000 rpm) for 90 min at 4°C (Sonics & Materials INC, USA/VCX500; Centrifuge 5804 Eppendorf AG. 22331, Hamburg, Germany); the supernatant was subjected to purification and the pellet was discarded.

Purification of CD2AP

The cell-free lysate was added to a Ni-NTA Sepharose (His Trap prepacked column by Cytiva) column equilibrated with 20 mM potassium phosphate buffer. After washing, the bound protein was eluted with 20 mM Potassium phosphate buffer (pH-7.6) containing 300 mM NaCl, 0.4 M Imidazole, and 5% glycer-

ol (**Figure 1B**). The purified protein was then dialyzed against buffer A to remove imidazole. The absorbance of the eluted fractions was recorded using a Jasco V-630 UV-vis spectrophotometer at 280 nm. A theoretical extinction coefficient value of 43890 M^{-1} cm^{-1} for CD2AP was used to determine the concentration of the purified CD2AP protein.

Analytical size exclusion chromatography

The oligomeric nature of CD2AP was initially determined by injecting 200 µl of 13.6 µM protein into a Superdex 200 Increase 10/300 column (Cytiva), connected to the NGC system (Bio-Rad). The column was pre-equilibrated with SEC buffer (50 mM Tris-HCl, 300 mM NaCl, 4 mM EGTA, 5 mM KCl, and 7% glycerol, pH 7.6). The peak fractions were collected and analyzed by SDS-PAGE. The oligomeric nature of CD2AP was further determined by injecting 200 µl of 13.6 µM protein into a Superose 6 Increase 10/300 column (Cytiva), connected to the NGC system (Bio-Rad). This column was pre-equilibrated with the same SEC buffer. The peak fractions were again collected and analyzed by SDS-PAGE. Additionally, to validate the SEC profile of CD2AP, the Superose 6 Increase 10/300 column was loaded with blue dextran to estimate the column's void volume.

Blue-native PAGE

Blue-Native (BN) PAGE was performed using the Native PAGÉ system (Invitrogen) according to the manufacturer's protocol. BN-PAGE was performed at 4°C by loading 30-40 µg of affinity-purified CD2AP onto a 6% gel using 1.5 M Tris-HCl pH 8.8 and Coomassie blue G250 (Himedia). Two running buffers were used: the cathode buffer (0.05% G250, 118 mM Tris-HCl, 39 mM Glycine) and the anode buffer (Tris-Glycine pH 8.0). The sample was prepared by mixing the purified protein with 5X dye (20% glycerol, 0.2 M Tris-HCl pH 6.8, 0.05% Bromophenol blue, 1% Triton X-100, and 0.25% G-250). The gel was run at 150 V at 4°C until the dye front was released. The gel was then stained with Coomassie blue R-250 (SRL), for visualization.

Circular dichroism spectroscopy

The circular dichroism (CD) spectra of recombinant CD2AP were recorded on a JASCO J-1500 CD spectrophotometer equipped with a thermoelectric (Peltier) cell holder. A protein concentration of 5.46 µM was used to obtain the far-UV CD spectrum. The far-UV (260-195 nm) CD measurements of CD2AP were recorded using a 0.2 cm path length cell at 2.5 nm bandwidth and a scan speed of 50 nm/min. The near-UV (260-360) CD measurements were recorded for the protein sample (25 µM) using a 0.5 cm path length cell at the bandwidth of 2.5 nm and a scan speed of 100 nm/min. We subsequently analyzed the effect of thermally induced unfolding and the stability of the secondary structural elements in CD2AP. The protein sample was subjected to a steady increase in temperature, and spectra were recorded in the far-UV region at intervals of 5°C using the same parameters.

Fluorescence spectroscopy

Intrinsic fluorescence measurements were collected on Jasco FP-6300 (Japan) equipped with an intense xenon flash lamp as the light source. An excitation wavelength of 286 nm was used, and the emission spectrum of CD2AP was obtained over a spectral range of 300-450 nm. We next assessed the tertiary packing integrity of CD2AP by measuring the change in fluorescence emission at 339 nm for every 5°C rise in temperature. A bandwidth of 2.5 nm and a scan speed of 200 nm/min was used, and the obtained spectra were corrected against the buffer. Quantitative analyses were performed using Origin Pro-version2020b (Origin Lab Corporation, Northampton, MA). A protein concentration of 5.46 µM was used for all fluorescence measurements. Refolding experiments of CD2AP were also carried out. Initially, the sample was heated to the maximum temperature of 95°C and then gradually cooled. As it cooled, the intrinsic tryptophan fluorescence was recorded at different temperatures. Furthermore, the tertiary packing integrity of CD2AP was assessed by treating the protein with varying concentrations of urea (0.1 M to 6 M). The data is included in the supplementary files of the manuscript (Supplementary Figure 3).

AlphaFold predictions

The predicted structure and sequence of CD2AP were obtained from the Alpha Fold database (www.alphafold.ebi.ac.uk) [54] and the

Uniprot database (Uniprot ID: Q9Y5K6), respectively. Structural prediction of wild-type and mutant tetrameric CD2AP was obtained using Alpha Fold Multimer via Cosmic2 [55]. While predicting the tetrameric models of the mutant CD2AP (p.K579Efs*7), the amino acids 587-639 were excluded. Default program parameters were used for the predictions. The program outputs provided five ranked models for the wild-type and mutant tetramers of CD2AP. A single subunit of the predicted wild-type tetramer was aligned with the retrieved monomer, and RMSD was calculated in PyMOL. Both the wild-type and mutant tetramers were also subjected to RMSD calculation post-alignment in PyMOL. We predicted the interactions within the modeled tetramers using Protein Interaction Analysis v2 in Maestro (Schrodinger release 2021-2).

Acknowledgements

The authors thank the DST-FIST and DBT-BUILDER facilities of the Department of Biochemistry and School of Life Sciences, UoH, Hyderabad. Also, we would like to thank Ms. Dagumati Praghna for making the schematic figures.

Disclosure of conflict of interest

None.

Address correspondence to: Abrar H Qadri and Anil K Pasupulati, Department of Biochemistry, School of Life Sciences, University of Hyderabad, Room F-73, Hyderabad 500046, India. Tel: +91-40-23134519; E-mail: syeduok@gmail.com (AHQ); anilkumar@uohyd.ac.in (AKP)

References

[1] Anil Kumar P, Welsh GI, Saleem MA and Menon RK. Molecular and cellular events mediating glomerular podocyte dysfunction and depletion in diabetes mellitus. Front Endocrinol (Lausanne) 2014; 5: 151.

[2] Imenez Silva PH and Mohebbi N. Kidney metabolism and acid-base control: back to the basics. Pflugers Arch 2022; 474: 919-934.

[3] Dhondup T and Qian Q. Acid-base and electrolyte disorders in patients with and without chronic kidney disease: an update. Kidney Dis (Basel) 2017; 3: 136-148.

[4] Cargill K and Sims-Lucas S. Metabolic requirements of the nephron. Pediatr Nephrol 2020; 35: 1-8.

[5] Grahammer F, Schell C and Huber TB. The podocyte slit diaphragm--from a thin grey line to a complex signalling hub. Nat Rev Nephrol 2013; 9: 587-598.

[6] Greka A and Mundel P. Cell biology and pathology of podocytes. Annu Rev Physiol 2012; 74: 299-323.

[7] Ebefors K, Lassen E, Anandakrishnan N, Azeloglu EU and Daehn IS. Modeling the glomerular filtration barrier and intercellular crosstalk. Front Physiol 2021; 12: 689083.

[8] Cortinovis M, Perico N, Ruggenenti P, Remuzzi A and Remuzzi G. Glomerular hyperfiltration. Nat Rev Nephrol 2022; 18: 435-451.

[9] Grahammer F, Schell C and Huber TB. Molecular understanding of the slit diaphragm. Pediatr Nephrol 2013; 28: 1957-1962.

[10] Kawachi H and Fukusumi Y. New insight into podocyte slit diaphragm, a therapeutic target of proteinuria. Clin Exp Nephrol 2020; 24: 193-204.

[11] Reiser J and Altintas MM. Podocytes. F1000Res 2016; 5: F1000 Faculty Rev-114.

[12] Grahammer F. New structural insights into podocyte biology. Cell Tissue Res 2017; 369: 5-10.

[13] Grahammer F, Wigge C, Schell C, Kretz O, Patrakka J, Schneider S, Klose M, Kind J, Arnold SJ, Habermann A, Brauniger R, Rinschen MM, Volker L, Bregenzer A, Rubbenstroth D, Boerries M, Kerjaschki D, Miner JH, Walz G, Benzing T, Fornoni A, Frangakis AS and Huber TB. A flexible, multilayered protein scaffold maintains the slit in between glomerular podocytes. JCI Insight 2016; 1: e86177.

[14] Daehn IS and Duffield JS. The glomerular filtration barrier: a structural target for novel kidney therapies. Nat Rev Drug Discov 2021; 20: 770-788.

[15] Fukasawa H, Bornheimer S, Kudlicka K and Farquhar MG. Slit diaphragms contain tight junction proteins. J Am Soc Nephrol 2009; 20: 1491-1503.

[16] Li C, Ruotsalainen V, Tryggvason K, Shaw AS and Miner JH. CD2AP is expressed with nephrin in developing podocytes and is found widely in mature kidney and elsewhere. Am J Physiol Renal Physiol 2000; 279: F785-792.

[17] Schwarz K, Simons M, Reiser J, Saleem MA, Faul C, Kriz W, Shaw AS, Holzman LB and Mundel P. Podocin, a raft-associated component of the glomerular slit diaphragm, interacts with CD2AP and nephrin. J Clin Invest 2001; 108: 1621-1629.

[18] Shih NY, Li J, Cotran R, Mundel P, Miner JH and Shaw AS. CD2AP localizes to the slit diaphragm and binds to nephrin via a novel C-terminal domain. Am J Pathol 2001; 159: 2303-2308.

[19] Dryer SE and Reiser J. TRPC6 channels and their binding partners in podocytes: role in glo-

merular filtration and pathophysiology. Am J Physiol Renal Physiol 2010; 299: F689-701.
[20] Kravets I and Mallipattu SK. The role of podocytes and podocyte-associated biomarkers in diagnosis and treatment of diabetic kidney disease. J Endocr Soc 2020; 4: bvaa029.
[21] Barletta GM, Kovari IA, Verma RK, Kerjaschki D and Holzman LB. Nephrin and Neph1 co-localize at the podocyte foot process intercellular junction and form cis hetero-oligomers. J Biol Chem 2003; 278: 19266-19271.
[22] Kocylowski MK, Aypek H, Bildl W, Helmstadter M, Trachte P, Dumoulin B, Wittosch S, Kuhne L, Aukschun U, Teetzen C, Kretz O, Gaal B, Kulik A, Antignac C, Mollet G, Kottgen A, Gocmen B, Schwenk J, Schulte U, Huber TB, Fakler B and Grahammer F. A slit-diaphragm-associated protein network for dynamic control of renal filtration. Nat Commun 2022; 13: 6446.
[23] Mulukala SKN, Kambhampati V, Qadri AH and Pasupulati AK. Evolutionary conservation of intrinsically unstructured regions in slit-diaphragm proteins. PLoS One 2021; 16: e0254917.
[24] Huber TB, Hartleben B, Kim J, Schmidts M, Schermer B, Keil A, Egger L, Lecha RL, Borner C, Pavenstadt H, Shaw AS, Walz G and Benzing T. Nephrin and CD2AP associate with phosphoinositide 3-OH kinase and stimulate AKT-dependent signaling. Mol Cell Biol 2003; 23: 4917-4928.
[25] Inoue K and Ishibe S. Podocyte endocytosis in the regulation of the glomerular filtration barrier. Am J Physiol Renal Physiol 2015; 309: F398-405.
[26] Tian X, Bunda P and Ishibe S. Podocyte endocytosis in regulating the glomerular filtration barrier. Front Med (Lausanne) 2022; 9: 801837.
[27] Yaddanapudi S, Altintas MM, Kistler AD, Fernandez I, Moller CC, Wei C, Peev V, Flesche JB, Forst AL, Li J, Patrakka J, Xiao Z, Grahammer F, Schiffer M, Lohmuller T, Reinheckel T, Gu C, Huber TB, Ju W, Bitzer M, Rastaldi MP, Ruiz P, Tryggvason K, Shaw AS, Faul C, Sever S and Reiser J. CD2AP in mouse and human podocytes controls a proteolytic program that regulates cytoskeletal structure and cellular survival. J Clin Invest 2011; 121: 3965-3980.
[28] Gigante M, Pontrelli P, Montemurno E, Roca L, Aucella F, Penza R, Caridi G, Ranieri E, Ghiggeri GM and Gesualdo L. CD2AP mutations are associated with sporadic nephrotic syndrome and focal segmental glomerulosclerosis (FSGS). Nephrol Dial Transplant 2009; 24: 1858-1864.
[29] Kiffel J, Rahimzada Y and Trachtman H. Focal segmental glomerulosclerosis and chronic kidney disease in pediatric patients. Adv Chronic Kidney Dis 2011; 18: 332-338.
[30] Tsvetkov D, Hohmann M, Anistan YM, Mannaa M, Harteneck C, Rudolph B and Gollasch M. A CD2AP mutation associated with focal segmental glomerulosclerosis in young adulthood. Clin Med Insights Case Rep 2016; 9: 15-19.
[31] Tapia C and Bashir K. Nephrotic Syndrome. In: StatPearls. Treasure Island (FL): StatPearls Publishing; 2023.
[32] Zhang A and Huang S. Progress in pathogenesis of proteinuria. Int J Nephrol 2012; 2012: 314251.
[33] Kim JM, Wu H, Green G, Winkler CA, Kopp JB, Miner JH, Unanue ER and Shaw AS. CD2-associated protein haploinsufficiency is linked to glomerular disease susceptibility. Science 2003; 300: 1298-1300.
[34] Liu YX, Zhang AQ, Luo FM, Sheng Y, Wang CY, Dong Y, Fan L and Liu L. Case report: a novel heterozygous mutation of CD2AP in a Chinese family with proteinuria leads to focal segmental glomerulosclerosis. Front Pediatr 2021; 9: 687455.
[35] Adair BD, Altintas MM, Moller CC, Arnaout MA and Reiser J. Structure of the kidney slit diaphragm adapter protein CD2-associated protein as determined with electron microscopy. J Am Soc Nephrol 2014; 25: 1465-1473.
[36] Zhang H, Lin L, Liu J, Pan L, Lin Z, Zhang M, Zhang J, Cao Y, Zhu J and Zhang R. Phase separation of MAGI2-mediated complex underlies formation of slit diaphragm complex in glomerular filtration barrier. J Am Soc Nephrol 2021; 32: 1946-1960.
[37] Zhou TB. Signaling pathways of PAX2 and its role in renal interstitial fibrosis and glomerulosclerosis. J Recept Signal Transduct Res 2012; 32: 298-303.
[38] Lehtonen S, Zhao F and Lehtonen E. CD2-associated protein directly interacts with the actin cytoskeleton. Am J Physiol Renal Physiol 2002; 283: F734-743.
[39] Grunkemeyer JA, Kwoh C, Huber TB and Shaw AS. CD2-associated protein (CD2AP) expression in podocytes rescues lethality of CD2AP deficiency. J Biol Chem 2005; 280: 29677-29681.
[40] Shaw AS and Miner JH. CD2-associated protein and the kidney. Curr Opin Nephrol Hypertens 2001; 10: 19-22.
[41] Mulukala Narasimha SK, Kar PP, Vadrevu R and Pasupulati AK. Intrinsically disordered regions mediate macromolecular assembly of the Slit diaphragm proteins associated with Nephrotic syndrome. Molecular Simulation 2019; 45: 603-613.
[42] Trivedi R and Nagarajaram HA. Intrinsically disordered proteins: an overview. Int J Mol Sci 2022; 23: 14050.
[43] Uversky VN. Intrinsically disordered proteins and their environment: effects of strong dena-

turants, temperature, pH, counter ions, membranes, binding partners, osmolytes, and macromolecular crowding. Protein J 2009; 28: 305-325.
[44] Uversky VN. Unusual biophysics of intrinsically disordered proteins. Biochim Biophys Acta 2013; 1834: 932-951.
[45] Wright PE and Dyson HJ. Intrinsically unstructured proteins: re-assessing the protein structure-function paradigm. J Mol Biol 1999; 293: 321-331.
[46] Wright PE and Dyson HJ. Linking folding and binding. Curr Opin Struct Biol 2009; 19: 31-38.
[47] Jarvet J, Damberg P, Danielsson J, Johansson I, Eriksson LE and Graslund A. A left-handed 3(1) helical conformation in the Alzheimer Abeta(12-28) peptide. FEBS Lett 2003; 555: 371-374.
[48] Malm J, Jonsson M, Frohm B and Linse S. Structural properties of semenogelin I. FEBS J 2007; 274: 4503-4510.
[49] Dyson HJ and Wright PE. Intrinsically unstructured proteins and their functions. Nat Rev Mol Cell Biol 2005; 6: 197-208.
[50] Habchi J, Tompa P, Longhi S and Uversky VN. Introducing protein intrinsic disorder. Chem Rev 2014; 114: 6561-6588.
[51] Kjaergaard M, Norholm AB, Hendus-Altenburger R, Pedersen SF, Poulsen FM and Kragelund BB. Temperature-dependent structural changes in intrinsically disordered proteins: formation of alpha-helices or loss of polyproline II? Protein Sci 2010; 19: 1555-1564.
[52] Uversky VN. Intrinsic disorder-based protein interactions and their modulators. Curr Pharm Des 2013; 19: 4191-4213.
[53] Mulukala SKN, Irukuvajjula SS, Kumar K, Garai K, Venkatesu P, Vadrevu R and Pasupulati AK. Structural features and oligomeric nature of human podocin domain. Biochem Biophys Rep 2020; 23: 100774.
[54] Jumper J, Evans R, Pritzel A, Green T, Figurnov M, Ronneberger O, Tunyasuvunakool K, Bates R, Zidek A, Potapenko A, Bridgland A, Meyer C, Kohl SAA, Ballard AJ, Cowie A, Romera-Paredes B, Nikolov S, Jain R, Adler J, Back T, Petersen S, Reiman D, Clancy E, Zielinski M, Steinegger M, Pacholska M, Berghammer T, Bodenstein S, Silver D, Vinyals O, Senior AW, Kavukcuoglu K, Kohli P and Hassabis D. Highly accurate protein structure prediction with AlphaFold. Nature 2021; 596: 583-589.
[55] Cianfrocco MA, Wong-Barnum M, Youn C, Wagner R and Leschziner A. COSMIC2: a science gateway for cryo-electron microscopy structure determination. Proceedings of the Practice and Experience in Advanced Research Computing 2017 on Sustainability, Success and Impact. 2017. pp. 1-5.

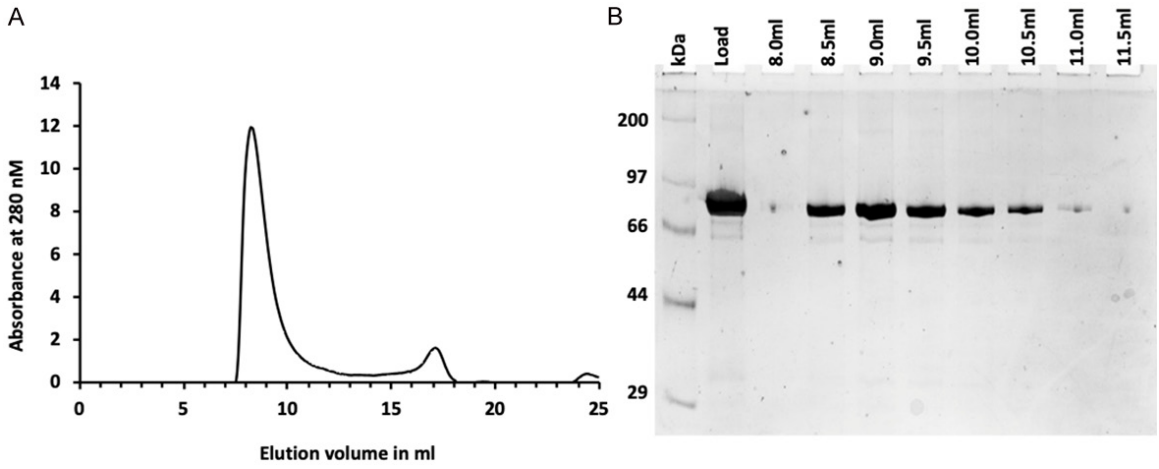

Supplementary Figure 1. SEC profile of CD2AP. A. Gel filtration chromatogram of CD2AP using superdex 200 increase 10/300 column from (Cytiva) showing CD2AP eluting at the void and elution volumes border. B. SDS-PAGE of the peak fractions collected from gel filtration chromatogram.

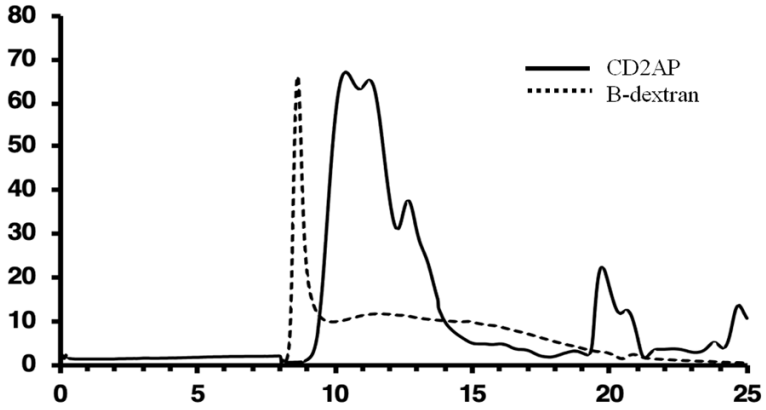

Supplementary Figure 2. SEC profile of CD2AP and blue dextran. The SEC profile of the purified CD2AP and blue dextran using superpose-6 increased 10/300 column (Cytiva), showing blue dextran in void volume and CD2AP in elution volume.

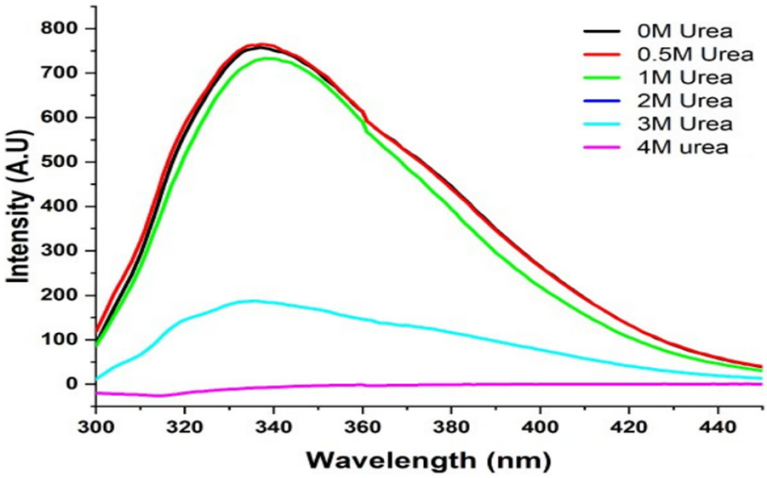

Supplementary Figure 3. Protein unfolding studies with urea. Intrinsic tryptophan fluorescence for CD2AP protein was measured with different urea concentrations by exciting the protein at 286 nm.

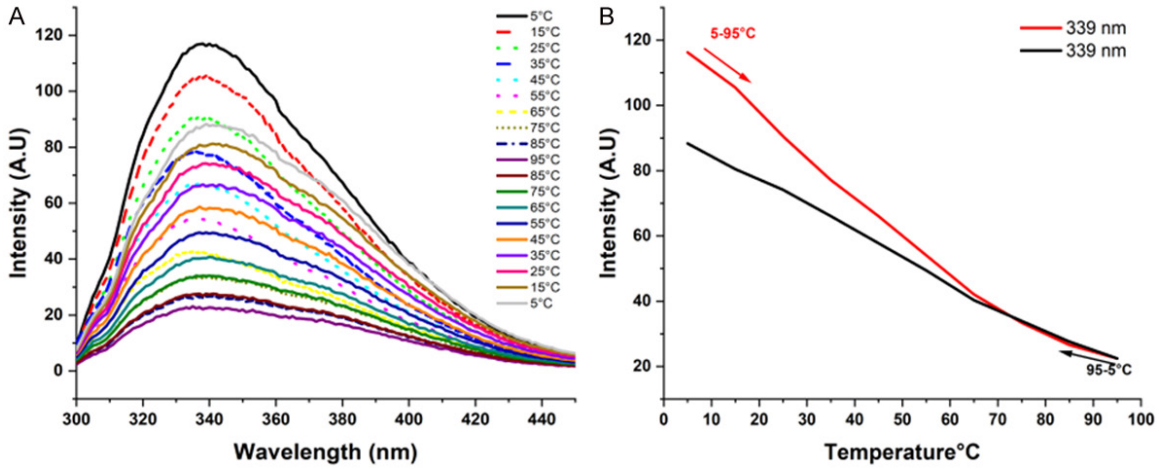

Supplementary Figure 4. Assessing the tertiary structural stability of the CD2AP oligomers. A. Intrinsic tryptophan fluorescence for CD2AP protein was measured as a function of temperature (5°C-90°C) and (back from 95°C to 5°C) by exciting the protein at 286 nm. B. Peak emission of the CD2AP protein at 339 nm is plotted over a temperature range of (5°C-90°C).